

Evidence for non-Gaussianity in the DMR Four Year Sky Maps

Pedro G. Ferreira ¹, João Magueijo², and Krzysztof M. Górski^{3,4}

¹Center for Particle Astrophysics, University of California, Berkeley, CA94720, USA

²Theoretical Physics, Imperial College, Prince Consort Road, London SW7 2BZ, UK

³Theoretical Astrophysics Center, Juliane Maries Vej 30, DK-2100, Copenhagen Ø,
Denmark

⁴Warsaw University Observatory, Warsaw, Poland

Received _____; accepted _____

ABSTRACT

We introduce and study the distribution of an estimator for the normalized bispectrum of the Cosmic Microwave Background (CMB) anisotropy. We use it to construct a goodness of fit statistic to test the coadded 53 and 90 GHz *COBE*-DMR 4 year maps for non-Gaussianity. Our results indicate that Gaussianity is ruled out at the confidence level in excess of 98%. This value is a lower bound, given all the investigated systematics. The dominant non-Gaussian contribution is found near the multipole of order $\ell = 16$. Our attempts to explain this effect as caused by the diffuse foreground emission from the Galaxy have failed. We conclude that unless there exists a microwave foreground emission which spatially correlates neither with the DIRBE nor Haslam maps, the cosmological CMB anisotropy is genuinely non-Gaussian.

Subject headings: Cosmology: theory – observation – the cosmic microwave background: tests of Gaussianity

1. Introduction

We shall consider fluctuations in the CMB as a random field on the sphere, $\frac{\Delta T}{T}(\mathbf{n})$. One can expand such a field in terms of Spherical Harmonic functions:

$$\frac{\Delta T}{T}(\mathbf{n}) = \sum_{\ell m} a_{\ell m} Y_{\ell m}(\mathbf{n}) \quad (1)$$

For a statistically isotropic field one has

$$\langle a_{\ell_1 m_1} a_{\ell_2 m_2}^* \rangle = C_{\ell_1} \delta_{\ell_1 \ell_2} \delta_{m_1 m_2} \quad (2)$$

We can also define the two-point function in terms of $\frac{\Delta T}{T}(\mathbf{n})$. Isotropy implies that the correlation matrix can only depend on the angle between the two points considered. This is encoded in the 2-point correlation $C^{(2)}(\theta)$. From (1) and (2) we find

$$C^{(2)}(\theta) = \sum_{\ell} \frac{2\ell + 1}{4\pi} C_{\ell} P_{\ell}(\cos \theta) \quad (3)$$

Hence the C_{ℓ} may be regarded as a Legendre transform of the 2-point correlation function.

It is a standard lore that, barring some mathematical obstructions, one can reconstruct the probability distribution function of any random field from its moments. Isotropy imposes “selection rules” on these moments. For instance, the 3-point moment is given by

$$\langle a_{\ell_1 m_1} a_{\ell_2 m_2} a_{\ell_3 m_3} \rangle = \begin{pmatrix} \ell_1 & \ell_2 & \ell_3 \\ m_1 & m_2 & m_3 \end{pmatrix} C_{\ell_1 \ell_2 \ell_3} \quad (4)$$

where the (...) is the Wigner $3J$ symbol. The coefficients $C_{\ell_1 \ell_2 \ell_3}$ are usually called the bispectrum. If we assume that there are no correlations between different ℓ multipoles then the only non-zero component of the bispectrum is $C_{\ell \ell \ell} = B_{\ell}$. The collapsed 3-point correlation function $C^{(3)}(\theta)$ (the average of a temperature squared at one point, and a temperature at another point, separated by an angle θ) is now

$$C^{(3)}(\theta) = \sum_{\ell} \left(\frac{2\ell + 1}{4\pi} \right)^{3/2} \begin{pmatrix} \ell & \ell & \ell \\ 0 & 0 & 0 \end{pmatrix} B_{\ell} P_{\ell}(\cos \theta) \quad (5)$$

in analogy with (3). Hence the B_ℓ is related to the Legendre transform of $C^{(3)}$. The angular power spectrum C_ℓ is often considered a more powerful tool than the correlation function $C^{(2)}(\theta)$ for discriminating between theories, and one might argue the same way with regard to the reduced bispectrum B_ℓ and the 3-point function $C^3(\theta)$.

The importance of higher order statistics for characterizing large scale structure has been stressed before (Peebles 1980). The non-linear evolution of primordial Gaussian fluctuations has been analysed in detail (Peebles 1980, Bouchet et al. 1992) and the skewness arising in such models has been shown to be consistent with current observations (Bouchet et al. 1993, Gaztañaga 1994). Luo 1994 discussed the statistical properties and detectability of the bispectrum for a variety of non-Gaussian signals. Kogut et al. (1996) measured the pseudocollapsed and equilateral three point function of the DMR four year data and found them to be consistent with Gaussianity. The analysis performed here should be considered complementary to that of Kogut et al. (1996): non-Gaussian signals which may be obscured in real space can become evident in ℓ space.

In this letter we shall use a general formalism for generating estimators of higher order moments on a sphere (Ferreira, Górski & Magueijo 1998). In this formalism one considers all possible tensor products of ΔT_ℓ (each multipole component of the field) and from these one extracts the singlet (invariant) term. In the case of bispectrum one has

$$\begin{aligned} \hat{B}_\ell &= \alpha_\ell \sum_{m_1 m_2 m_3} \begin{pmatrix} \ell & \ell & \ell \\ m_1 & m_2 & m_3 \end{pmatrix} a_{\ell m_1} a_{\ell m_2} a_{\ell m_3} \\ \alpha_\ell &= \frac{1}{(2\ell + 1)^{\frac{3}{2}}} \begin{pmatrix} \ell & \ell & \ell \\ 0 & 0 & 0 \end{pmatrix}^{-1} \end{aligned} \quad (6)$$

Note that only even values of ℓ lead to nonzero values of the \hat{B}_ℓ due to the symmetries of the Wigner 3-J coefficients. In practice it is essential to factor out the power spectrum from our statistic. We also wish to define statistics which are invariant under parity transformations,

and not just rotations. Therefore we define I_ℓ^3 to be

$$I_\ell^3 = \left| \frac{\hat{B}_\ell}{(\hat{C}_\ell)^{3/2}} \right| \quad (7)$$

where $\hat{C}_\ell = \frac{1}{2\ell+1} \sum_m |a_{\ell m}|^2$. Our statistics are dimensionless and are normalized so that a cylindrically symmetric multipole has $I_\ell^3 = 1$.

The $\ell = 2$ case was discussed and given a physical interpretation in Magueijo (1995). The quadrupole has 5 degrees of freedom. Of these only 2 are rotationally invariant. One is the quadrupole intensity C_2 , and tells us how much power there is in the quadrupole. The other is essentially I_2^3 and tells us how this power is distributed among the different a_{2m} but only as far as there is a rotationally invariant meaning to the concept. For instance if $I_2^3 = 1$ then there is a frame in which all the power is concentrated in the $m = 0$ mode. Such a quadrupole is cylindrically symmetric, but of course the symmetry axis orientation is uniformly distributed, to comply with statistical isotropy. If $I_2^3 = 0$ then on the contrary cylindrical symmetry is maximally broken. The probability distribution function of I_2^3 is uniform in Gaussian theories (Magueijo (1995)).

2. Goodness of fit and evidence for non-Gaussianity

We will be testing the inverse noise variance weighted, average maps of the 53A, 53B, 90A and 90B *COBE*-DMR channels, with monopole and dipole removed, at resolution 6, in ecliptic pixelization. We use the extended galactic cut of Banday et al 1997, and Bennet et al 1996 to remove most of the emission from the plane of the Galaxy. We apply our statistics to the DMR maps before and after correction for the plausible diffuse foreground emission outside the galactic plane as described in Kogut et al. (1996), and Górski et al. 1996. To estimate the I_ℓ^3 s we set the value of the pixels within the galactic cut to 0 and the average temperature of *the cut map* to zero. We then integrate the map multiplied with

spherical harmonics to obtain the estimates of the $a_{\ell m}$ s and apply equations 6 and 7.

We have used Monte Carlo simulations to find the distribution of the estimators I_ℓ^3 as applied to Gaussian maps subject to DMR noise and galactic cut (see Fig. 1). These distributions are very non-Gaussian. In principle this would complete the theoretical work required for converting the observed I_ℓ^3 (which we also plot in Fig. 1) into a statistical statement on Gaussianity, but we proceed further by defining a new “goodness of fit” statistic as follows.

We wish to construct a tool similar to the χ^2 (often used for comparing predicted and observed C_ℓ spectra) but adapted to the non-Gaussian distributions $P(I_\ell^3)$. First, however, recall that if the $\{I_\ell^3\}$ were a set of N independent, $N(\mu_\ell, \sigma_\ell)$ -distributed variables, the usual definition of the chi squared would read

$$X^2 = \frac{1}{N} \sum \frac{(I_\ell^3 - \mu_\ell)^2}{\sigma_\ell^2}, \quad (8)$$

with X^2 distributed as χ_N^2 , a good fit represented by $X^2 \approx 1$, and $X^2 \ll 1$ ($X^2 \gg 1$) corresponding to the unusually large (small) scatter in the data given the assumed variances. The distribution of X^2 is used to find the probability, given the model, of a value of X^2 as large or as small as the one observed. The converse probability is the confidence level for rejecting the model.

Since the I_ℓ^3 distributions are non Gaussian we generalize the χ^2 for a set of probability functions $P_\ell(I_\ell^3)$ associated with observations $\{I_\ell^3\}$ by defining the following functional

$$X^2 = \frac{1}{N} \sum_\ell X_\ell^2 = \frac{1}{N} \sum_\ell (-2 \log P_\ell(I_\ell^3) + \beta_\ell), \quad (9)$$

where the constants β_ℓ are defined so that for each term of the sum $\langle X_\ell^2 \rangle = 1$. The definition reduces to the usual X^2 for Gaussian P_ℓ .

As an illustration let us first approximate the distributions of the I_ℓ^3 by $P(I_\ell^3) = 2(1 - I_\ell^3)$ — a good approximation for ℓ around 10. Then $X^2 = -2 \log(1 - I_\ell^3)$. Like the standard X^2

one has $0 < X^2 \ll 1$ for observations close to the peak of the distribution, here at $I_\ell^3 = 0$. Indeed $X^2(0) = 0$. However the peak of $P(I_\ell^3)$ is far from its average, and so the standard X^2 would produce $X^2 = 0$ at the wrong observation. For observations far from the peak of the distribution (but subject to the constraint $I_\ell^3 \leq 1$) X^2 goes to infinity. In contrast the standard X^2 would always remain finite.

The proposed X^2 therefore does for these non-Gaussian distributions what the usual X^2 does for normal distributions. To illustrate its efficiency let us find its distribution. First note that $P(X^2) = \exp(-X^2)$. Consider now a X_N^2 built from averaging the X^2 of N independent observations:

$$X_N^2 = \frac{-2}{N} \sum_{\ell} \log(1 - I_\ell^3) \quad (10)$$

Using characteristics its distribution may be found to be

$$F(X_N^2) = \frac{N^N}{(N-1)!} e^{-NX_N^2} X_N^{2N-2} \quad (11)$$

This is a χ_{2N}^2 . Even if the original invariants were Gaussian distributed the standard X^2 would only be a χ_N^2 . Of course for values of ℓ away from 10 the $P(I_\ell^3)$ are very different from the analytical fit presented. In particular for $\ell = 2$ the distribution is uniform, meaning that any observation is compatible with Gaussianity. Applying the prescription (9) we have that indeed $X^2(I_2^3) = 1$.

In practice we build a X^2 for the *COBE*-DMR data by means of Monte Carlo simulations. We proceed as follows. First we compute the distributions $P(I_\ell^3)$, for $\ell = 2, \dots, 18$, for a Gaussian process as measured subject to our galactic cut, and pixel noises. These $P(I_\ell^3)$ were inferred from 25000 realizations (see Fig. 1). From these distributions we then build the X^2 defined in (9), taking special care with the numerical evaluation of the constants β_ℓ . We call this function X_{COBE}^2 . We then find its distribution $F(X_{COBE}^2)$ from 10000 random realizations. This is very well approximated by a χ^2 distribution with 12 degrees of freedom. If all $P(I_\ell^3)$ were as in the analytical fit above,

we could conclude that we successfully measured an effective number of useful invariants equal to 6. This is less than the number of invariants we actually measured (10) and this is simply due to anisotropic noise and galactic cut. However, had we used a standard χ^2 statistics the effective number of useful invariants would be only 3.

We then compute X_{COBE}^2 with the actual observations and find $X_{COBE}^2 = 1.81$. One can compute $P(X_{COBE}^2 < 1.81) = 0.98$. Hence, it would appear that we can reject Gaussianity at the 98% confidence level.

3. Discussion

The result that we have obtained raises a number of questions which we shall attempt to answer. From Fig. 1 it is clear that I_{16}^3 is far in the tail of the Gaussian ensemble and it dominates the statistic. One would like to understand the importance of both cosmic variance and noise to this measurement. We would also like to assess the extent to which a galactic foreground contaminant could be responsible for this result.

In order to answer the first question we look for Bayesian estimates for the I_ℓ^3 as they are *for our sky*. To do this we first estimate what the temperature fluctuations $T_i = \frac{\Delta T}{T}(\mathbf{n}_i)$ in each pixel i in our dataset are likely to be, given DMR observations O_i , and noises σ_i^2 . We construct the posterior $P(T_i|O_i)$ assuming uniform priors in T_i , and also that a priori no correlations exist between the T_i . The latter assumption is often used in image restoration algorithms, such as maximum entropy methods. We then produce an ensemble of skies with the distribution $P(T_i|O_i)$. From it we infer $P(I_\ell^3|O_i)$, the distributions for what the I_ℓ^3 for our sky are likely to be given DMR observations and noise. This procedure will allow us to assess the importance of noise in each of our measurements. However note that this analysis is totally decoupled from the result in the previous section where all we need to

know are the observed I_ℓ^3 , not their estimates for our sky.

In Fig. 2 we plot in dotted lines $P(I_\ell^3|O_i)$ for our data set. We also plot in solid lines the cosmic variance distribution of I_ℓ^3 in skies with the same galactic cut. The vertical line is the observed invariant $I_\ell^3(O_i)$. As expected we see that, as ℓ gets larger, the spread in $P(I_\ell^3|O_i)$ due to noise becomes more important, at $\ell = 18$ dominating the distribution function. On the other hand we clearly have succeeded in making measurements for $\ell = 4, 6, 8, 12, 14, 16$. For them $P(I_\ell^3|O_i)$ are peaked and clearly different from the cosmic variance distribution. The fact that $P(I_{16}^3|O_i)$ does not peak at $I_{16}^3(O_i)$ is merely a failure of the prior. The measurement of $I_{16}^3(O_i)$ is therefore a signal and is not dominated by noise. We have further checked that the signal to noise in power at $\ell = 16$ is of order 1.

Next we wish to know if galactic emissions could be blamed for this result. We can proceed in three ways. Firstly we may use instead the DMR cosmic emission maps, where a linear combination of the various DMR channels is used to separate out the foreground Galactic contamination. In these maps the noise level is considerably higher. Plotting the counterpart of Fig. 2 for this case we find that the distributions of the actual I_ℓ^3 for our sky, given noise induced errors, are very similar to their cosmic variance distributions. The measurement is therefore dominated by noise and inconclusive. We find $X_{COBE}^2 = .4$, consistent with Gaussianity, but this is a mere check of the Gaussianity of noise. Hence this approach towards foregrounds turns into a dead end, but serves to show how large angle Gaussian tests is a field constrained by noise, not cosmic variance.

As an alternative approach we may subject galactic templates to the same analysis. At the observing frequencies the obvious contaminant should be foreground dust emission. The DIRBE maps (Boggess et al. 1992) supply us with a useful template on which we can measure the I_ℓ^3 s. We have done this for two of the lowest frequency maps, the 100 μm and the 240 μm maps. The estimate is performed in exactly the same way as for the DMR data

(i.e. using the extended Galaxy cut). We performed a similar exercise with the Haslam 408Mhz (Haslam (1982)) map. We display their values in Fig. 3. As expected the two maps have consistent values for the I_ℓ^3 . However they do not have a non-Gaussian value at $\ell = 16$. Indeed for all ℓ the I_ℓ^3 are within Gaussian cosmic variance error bars. This is not surprising. DIRBE maps exhibit structures on very small scales. These should average into a Gaussian field when subject to a 7° beam.

As a third alternative we may use foreground corrected maps. In these one corrects the coadded 53 and 90 Ghz maps for the DIRBE correlated emission. We have considered corrected maps in ecliptic and galactic frames, and also another map made in the ecliptic frame but with the DIRBE correction forced to have the same coupling as determined in the galactic frame. As shown in Fig. 3, in all of these the non-Gaussian signal at $\ell = 16$ is enhanced, although we observe large variations in I_ℓ^3 at $\ell = 4 - 8$ (a phenomenon noticed before when estimating C_ℓ -s). In fact the corrected maps exclude Gaussianity at the confidence level of 99.5%.

It would be interesting to relate our result to the curious dip in power at $\ell \approx 16$ provided by the maximum likelihood estimates in Górski (1997). These show that, *assuming a Gaussian signal*, the power in signal and noise is unusually low at $\ell \approx 16$. One wonders how this would be affected if non-Gaussian degrees of freedom were allowed into the estimation (Ferreira, Górski & Magueijo 1998).

We have also subjected our work to a variety of numerical tests. Arbitrary rotations of the coordinate system affects results to less than a part in 10^5 . More importantly, comparing data pixelized in the ecliptic and galactic frames, we found that our results were very robust, indeed more so than the power spectrum estimation (see the bottom pannel of Fig. 3). We also tried different galactic cuts, and found that although the non-Gaussian signal gets transferred to other ℓ , one does not fully erase it until a cut of $\pm 40^\circ$ is applied.

Finally we checked the effect of varying the offset in the cut map. We found that for any other prescription than the one used the effect is enhanced, often leading to rejecting Gaussianity at more than the 99.5% confidence level.

To conclude, we have not been able to attribute our result to a known contaminating source or a systematic. Indeed the confidence level quoted refers to the worst result obtained within the set of effects explored. Of course it is always possible that this non-Gaussian signal comes from some yet unmapped foreground, which cannot be separated from the CMB anisotropy signal in the *COBE*-DMR data — the poorly known free-free emission from the Galaxy comes to mind here.

If indeed our results are due to a foreground contamination one should note the following two points. First, we would have demonstrated that DMR data is more contaminated by foregrounds than thought before. Second, Galactic emissions on the scales considered are often assumed to be Gaussian. In fact this assumption is used in subtraction algorithms based on the idea of optimal filtering. The discovery of a distinctly non-Gaussian galactic emission would in the very least require a rethinking of the foreground subtraction algorithms.

If, on the other hand, the CMB signal itself is demonstrably non-Gaussian, we would not need to over-emphasise the epistemological implications of our findings.

Acknowledgements

We thank T. Banday, T. Bunn, K. Baskerville, M. Hobson, A.Jaffe, J.Nunes, D.Spergel and R.Taillet. Resources of Starlink (IC) and of the COMBAT collaboration were used in this project. PGF was supported by NSF (USA), JNICT (PORTUGAL) and CNRS (FRANCE), JM by the Royal Society and TAC, and KMG by Danmarks

Grundforskningsfond (TAC) and partly by NASA-ADP grant.

REFERENCES

- Banday, A.J., Górski, K.M., Bennett, C.L., Hinshaw, G., Kogut, A., Lineweaver, C., Smoot, G.F., and Tenorio, L. (1997) *Ap.J.*, **475**, 393
- Bennet, C.L., Banday, A.J., Górski, K.M., Hinshaw, G., Jackson, P.D., Keegstra, P., Kogut, A., Smoot, G.F., Wilkinosn, D.T., Wright, E. L. (1996) *Ap. J.* **464**, 1
- Bogess et al. (1992) *Ap. J* **397** 420
- Bouchet, F.R., Juskiwicz, R., Colombi, S., Pellat, R. (1992) *Ap. J. Lett.* **394**, L5
- Bouchet, F.R., Strauss, M., Davis, M., Fisher, K.B., Yahil, A., Huchra, J.P. (1993) *Ap. J.* **417**, 36
- Ferreira, P. G., Górski, K. M., Magueijo, J. (1998) in preparation
- Gaztañaga, E. (1994) *M.N.R.A.S.* **268**, L1.
- Górski, K. M., Hinshaw, G., Banday, A. J., Bennett, C. L., Wright, E. L., Kogut, A., Smoot, G. F., Lubin, P. (1996) *Ap. J. Lett.* **464**, L11
- Górski, K. M., in Microwave Background Anisotropies, Proceedings of the XVIth Moriond Astrophysics Meeting, March 1996, Editions Frontieres 1997; also astro-ph/9701191
- Haslam, C.G.T et al (1982) *Astron. Astrophys. Suppl. Ser.*, **63**, 205.
- Kogut, A., Banday, A. J., Bennett, C. L., Górski, K. M., Hinshaw, G., Smoot, G. F., Wright, E. L. (1996) *Ap. J.* **464** L29
- Kogut, A., Banday, A. J., Bennett, C. L., Górski, K. M., Hinshaw, G., Smoot, G. F., Wright, E. L. (1996) *Ap. J.* **464** L5
- Luo X. (1994) *Ap. J.* **427** L71.

Magueijo, J. (1995) *Phys. Lett.* **B342** 32-39 ERRATUM-ibid **B352** 499.

Peebles, P.J.E. (1980) *The Large Scale Structure of the Universe* (PUP, Princeton)

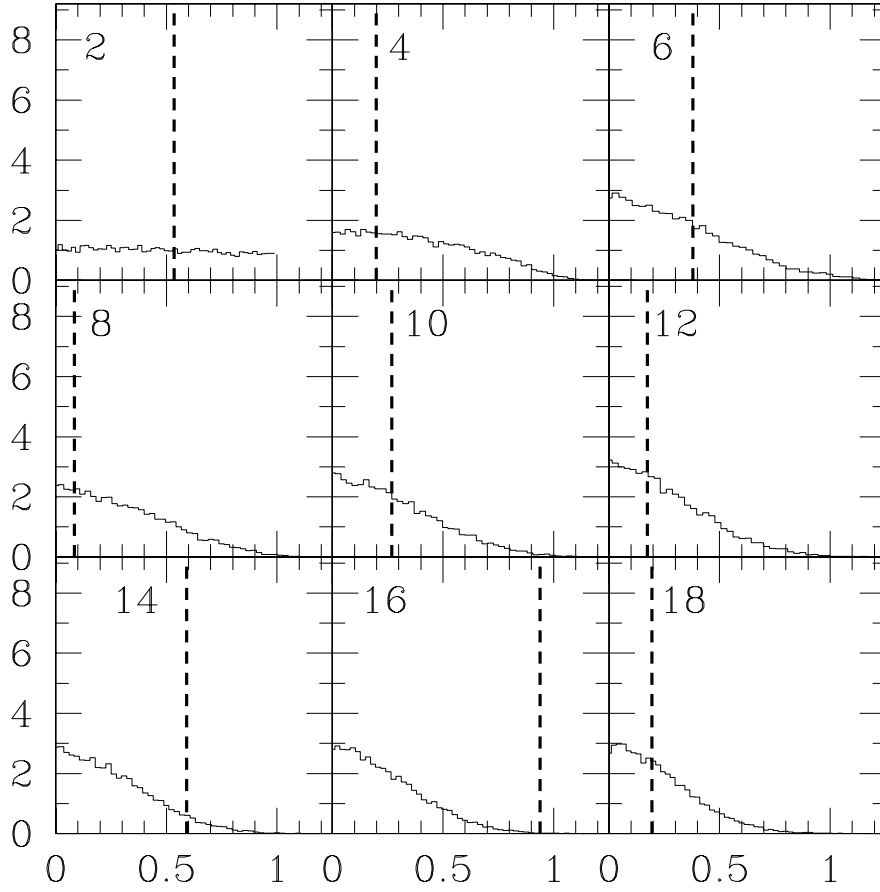


Fig. 1.— The vertical thick dashed line represents the value of the observed I_l^3 . The solid line is the probability distribution function of I_l^3 for a Gaussian sky with extended galactic cut and DMR noise.

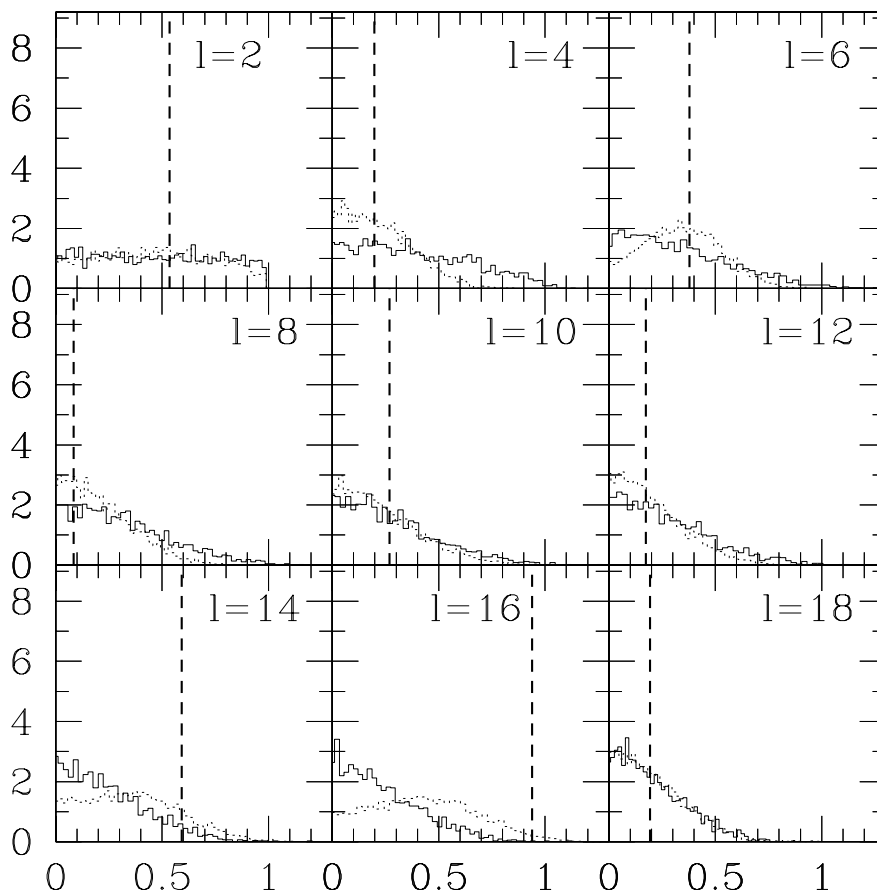


Fig. 2.— The vertical thick dashed line represents the value of the observed I_ℓ^3 , that is $I_\ell^3(O_i)$. The dotted line is the distribution of where the I_ℓ^3 for our sky are likely to be, given the observations O_i and noise, that is $P(I_\ell^3|O_i)$. The solid line is the cosmic variance distribution of I_ℓ^3 for a Gaussian process (subject to the same cut, but with no noise).

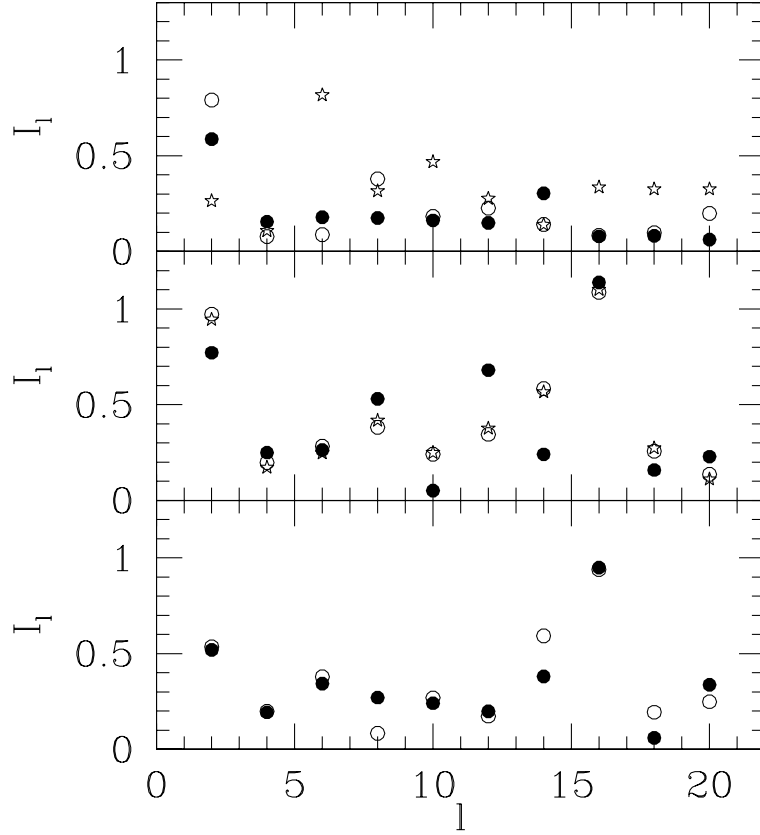


Fig. 3.— In the bottom panel we plot the measured I_ℓ from the data in ecliptic coordinates (open circles) and galactic coordinates (solid circles); the center panel has the foreground corrected data in ecliptic coordinates (open circles) and galactic coordinates (solid circles) and ecliptic coordinates with galactic frame coupling (stars); the top panel has the DIRBE $100\mu\text{m}$ (open circles) DIRBE $240\mu\text{m}$ (solid circles) and Haslam (stars) data.